Carbon Trends 4 (2021) 100068

Contents lists available at ScienceDirect

Carbon Trends

journal homepage: www.elsevier.com/locate/cartre

Comparison of carbonized and activated polypyrrole globules, nanofibers, and nanotubes as conducting nanomaterials and adsorbents of organic dye

Jaroslav Stejskal[a,*], Miroslava Trchová[b], Ladislav Lapčák[b], Zdeňka Kolská[c], Miroslav Kohl[d], Michal Pekárek[a], Jan Prokeš[e]

[a] Institute of Macromolecular Chemistry, Academy of Sciences of the Czech Republic, 162 06 Prague 6, Czech Republic
[b] University of Chemistry and Technology, Prague, 188 28 Prague 6, Czech Republic
[c] Faculty of Science, J.E. Purkyně University, 400 96 Ústí nad Labem, Czech Republic
[d] Faculty of Chemical Technology, University of Pardubice, 532 10 Pardubice, Czech Republic
[e] Faculty of Mathematics and Physics, Charles University, 180 00 Prague 8, Czech Republic

ARTICLE INFO

Article history:
Received 21 April 2021
Revised 25 May 2021
Accepted 29 May 2021

Keywords:
Conducting polymer
Polypyrrole
Nanotubes
Carbonization
Activation
Dye adsorption

ABSTRACT

Polypyrrole globules, nanofibers and nanotubes were activated by their carbonization at 650 °C in the 3:1 mass excess of molten potassium hydroxide in argon. They have been compared with parent polypyrroles and analogous samples obtained by the carbonization in the absence of hydroxide. The yields after activation, 12–18 wt%, were lower compared to the carbonization, which exceeded 50 wt%. The changes in molecular structure are discussed on the basis of FTIR and Raman spectra. One-dimensional morphologies, especially nanotubes, were superior to globules in most respects. They have higher conductivity close to 10 S cm^{-1}, which was reduced by two orders of magnitude after carbonization but partly recovered after activation. The specific surface areas of nanotubes of the order of tens m^2g^{-1} was several times higher compared with globules. They have not changed after carbonization but increased several times upon activation. The activated polypyrroles were tested as adsorbents of anionic azo dye, Reactive Black 5. Activated nanotubes performed the best in adsorption followed by parent nanotubes and nanofibers. The mechanism of dye adsorption is proposed by considering the presence of dye tautomers identified on the basis of FTIR spectra.

ORCID
Jaroslav Stejskal 0000-0001-9350-9647
Miroslava Trchová 0000-0001-6105-7578
Ladislav Lapčák 0000-0002-0498-5148
Miroslav Kohl 0000-0003-0054-6938
Zdeňka Kolská 0000-0003-0239-9046
Michal Pekárek 0000-0003-4953-5391
Jan Prokeš 0000-0002-8635-7056

1. Introduction

Polypyrrole is probably the most studied conducting polymer due to its electrical and electrochemical properties and its ability to respond to external stimuli. Various ways have been sought how to improve the conductivity [1] and the preparation of one-dimensional polypyrrole morphologies, nanofibers and nanotubes, is the most promising research direction in this respect. The preparation and applications of polypyrrole nanotubes has recently been reviewed [2]. It has been demonstrated that especially the presence of organic dyes introduced to the polypyrrole synthesis may convert the common globular morphology to one-dimensional objects [3,4]. Methyl orange has been routinely used for this purpose [5–12]. Only exceptionally other dyes, such as Acid Blue 25 [13] or safranin [14] have similarly been applied in the morphology control.

The special interest, however, has been paid also to the conversion of polypyrrole nanotubes to nitrogen-containing carbon analogues. The preparation and applications of carbonized conducting polymers have recently been reviewed [15]. The typical carbonization of polypyrrole takes place in inert atmosphere at temperatures 500–1000 °C for various times, the typical yields exceed 50 wt%

* Corresponding author.
E-mail address: stejskal@imc.cas.cz (J. Stejskal).

https://doi.org/10.1016/j.cartre.2021.100068

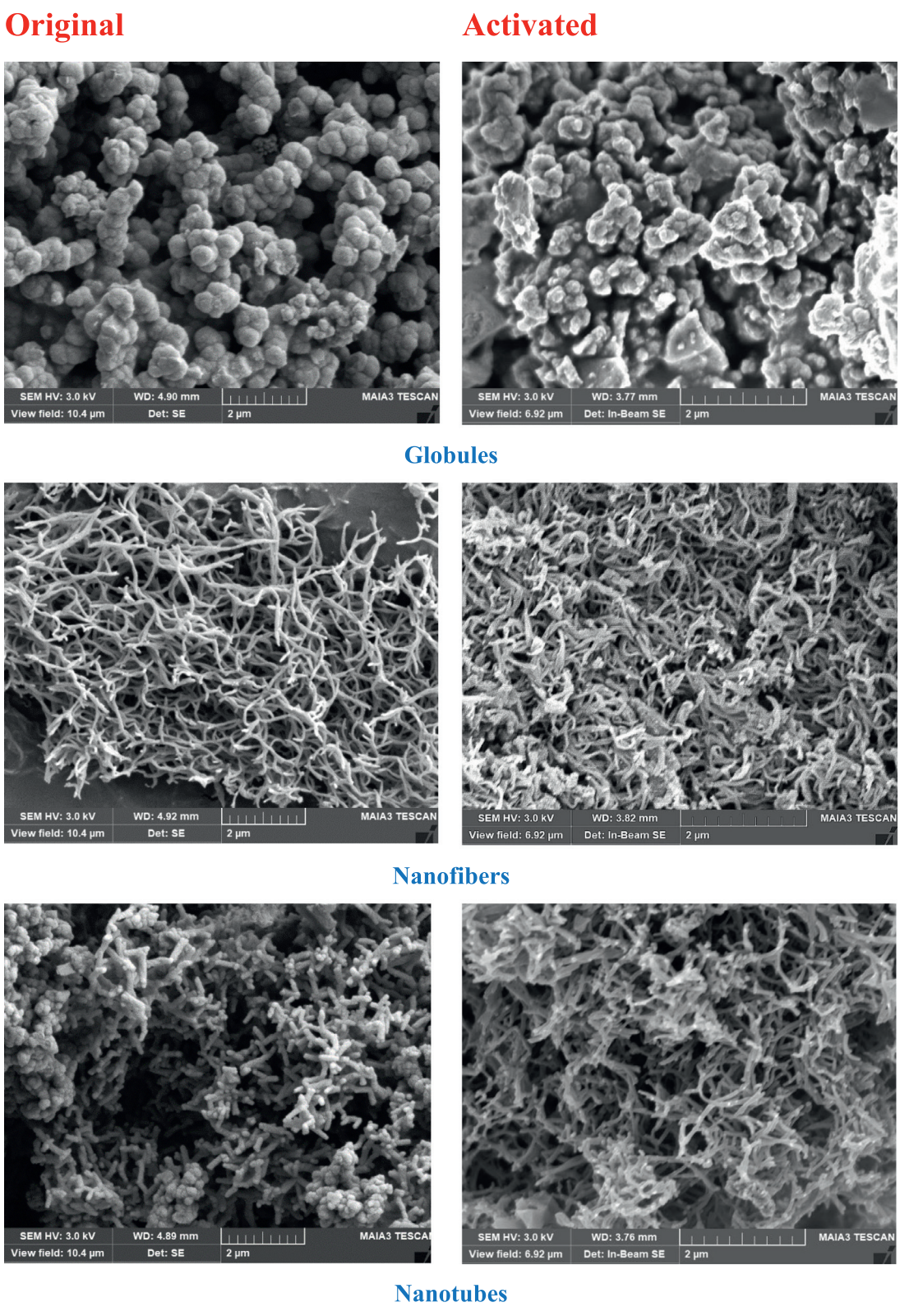

Fig. 1. Polypyrrole globules, nanofibers and nanotubes before (left) and after the activation (right). Scale bars 2 μm.

[4,16–18]. The morphology is retained after carbonization while the conductivity is reduced but not lost [4]. Carbonized polypyrrole nanotubes have been applied as electrodes in batteries [7] and supercapacitors [9,19], electrocatalysts in oxygen reduction reaction [20,21], catalysis of organic reductions [6], for adsorption of organic dyes [4,19] or water desalination [10].

Sometimes the so-called activation has been used as the carbonization tool in order to increase the specific surface area that is required by some applications, e.g., in energy-storage devices or adsorbents. In this process, either original conducting polymers or already carbonized ones are heated along with mass excess of potassium hydroxide [22], typically 2–4:1 by weight, in inert at-

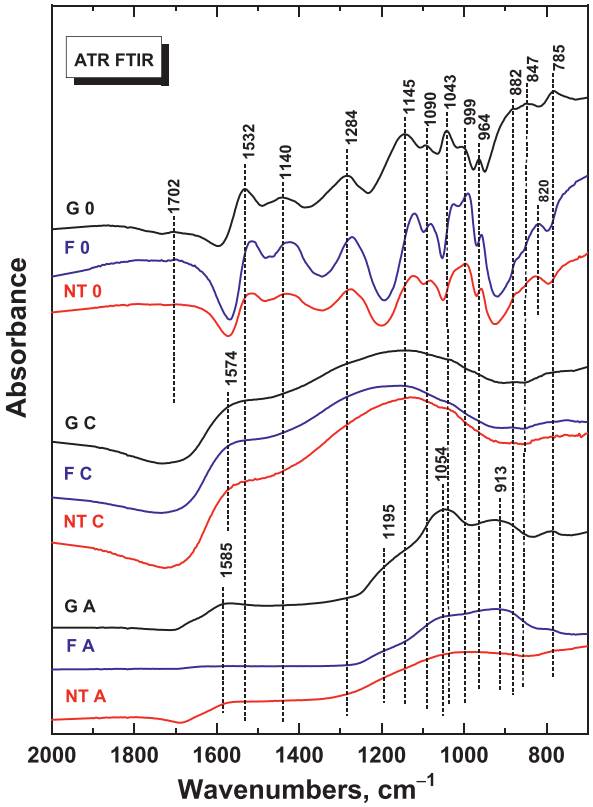

Fig. 2. ATR FTIR spectra of original (0), carbonized (C) and activated (A) polypyrrole globules (G), nanofibres (F) and nanotubes (NT).

mosphere at temperature above the melting point of the alkali, 360 °C, usually at 600–800 °C. Compared with the standard carbonization in inert atmosphere, the yields of the activated product are lower. Activated polypyrrole nanotubes have been tested as electrocatalysts in oxygen reduction reaction [23,24], in lithium ion [25] and lithium–sulfur batteries [26] and supercapacitor electrodes [27].

The present study compares the electrical and dye-adsorption properties of polypyrrole globules, nanofibers and nanotubes with the analogues obtained by the carbonization at 650 °C in inert atmosphere and activation at the same temperature in the presence of potassium hydroxide.

2. Experimental

2.1. Polypyrroles

Three polypyrroles with different morphology – globules, nanofibers and nanotubes – have been selected for the present study. Globular polypyrrole was prepared by the routine oxidation of 0.2 M pyrrole with 0.5 M iron(III) chloride in aqueous medium at room temperature [4] (Fig. 1). Polypyrrole nanofibers were synthesized similarly using 0.2 M pyrrole and 0.2 M iron(III) chloride in the presence of 0.01 M Acid Blue 25 dye [13]. Finally, polypyrrole nanotubes originated in the oxidation of 0.05 M pyrrole with 0.05 M iron(III) chloride along with 0.0025 M methyl orange (Acid Orange 52) [2,28,29]. All chemicals were purchased from Sigma-Aldrich. The details of the preparation and characterization of polypyrroles and their carbonization in inert atmosphere at 650 °C has recently been reported elsewhere [4]. The present study concentrates on the activation of these polypyrroles.

2.2. Activation

2 g of polypyrroles in quartz container were covered with *ca* 6 g of potassium hydroxide flakes (reagent grade, 90%; Sigma-Aldrich) and placed in the cylindrical furnace Clasic (Clasic CZ Ltd) under argon atmosphere. The temperature was increased at 5 °C min^{-1} rate to 650 °C and the samples were kept at this temperature for 1 h. The heating was then switched off and the sample was left to cool to room temperature still under argon. The products of activation were suspended in 100 mL of water and separated after 24 h by filtration. The solids were rinsed with 50 mL 0.1 M hy-

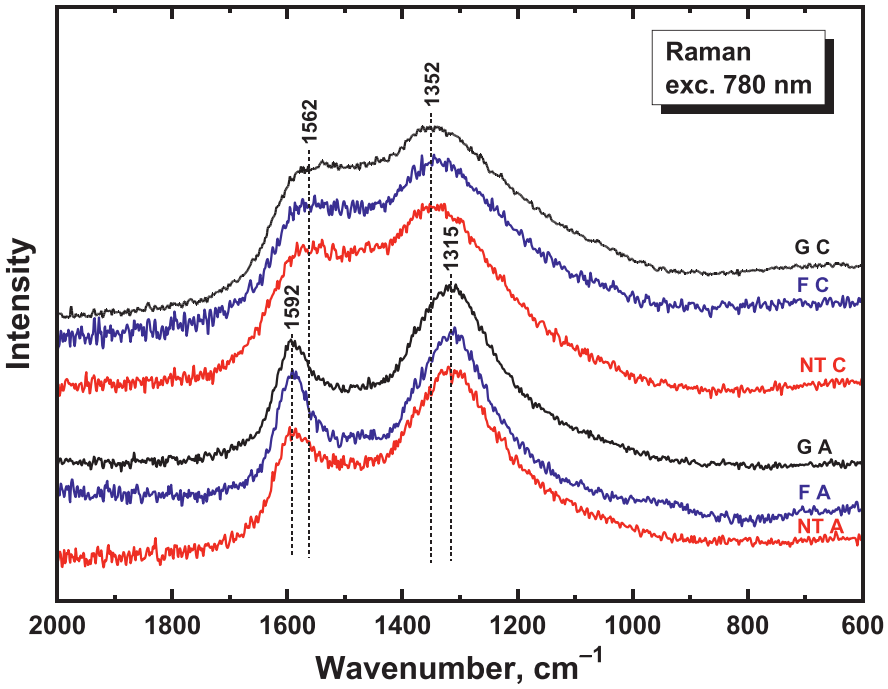

Fig. 3. Raman spectra of carbonized (C) and activated (A) polypyrrole globules (G), nanofibres (F) and nanotubes (NT).

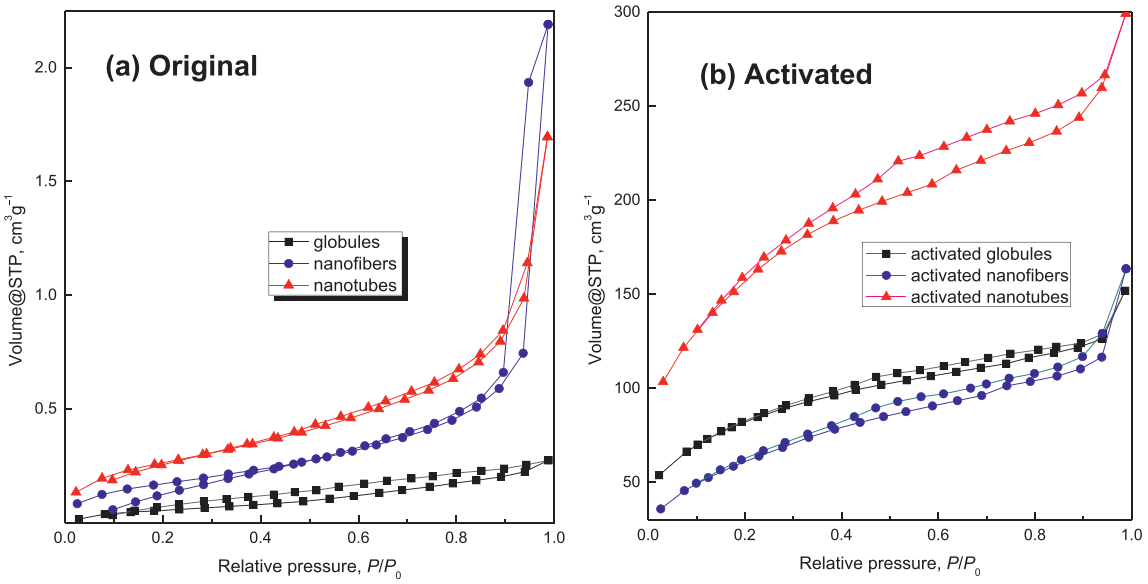

Fig. 4. Adsorption/desorption isotherms of (a) original [4] and (b) activated polypyrroles.

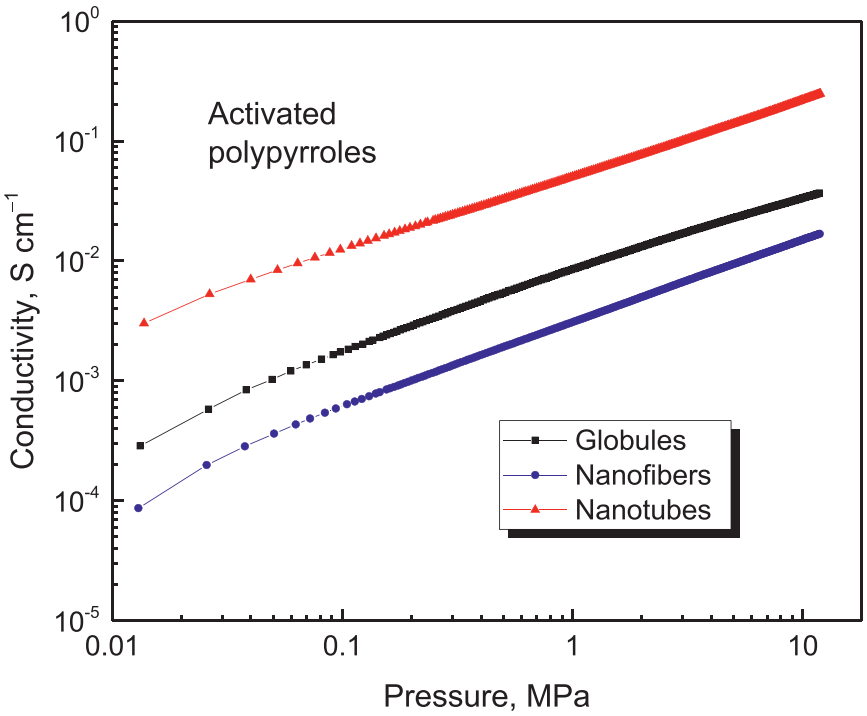

Fig. 5. Conductivity of activated polypyrroles in dependence on pressure.

drochloric acid to neutralize any residual hydroxide and then by water to neutral reaction. The activated polypyrrole was left to dry at room temperature and then in air at 100 °C. The yields were 0.25 g (12.5 wt%), 0.35 g (17.5 wt%), and 0.35 g (17.5 wt%) for globules, nanofibers, and nanotubes, respectively.

2.3. Characterization

Morphology was observed with a scanning ultra-high-resolution electron microscope MAIA3 Tescan (Czech Republic). Elemental analysis of the samples has been reported elsewhere [4].

ATR FTIR spectra of the powdered samples were recorded using Nicolet 6700 spectrometer (Thermo Scientific, Madison, WI, USA) in a dry air-purged environment equipped with reflective ATR extension GladiATR (PIKE Technologies, USA) with diamond crystal. Spectra were recorded in the 4000–400 cm^{-1} region with DLaTGS (deuterated L-alanine-doped triglycine sulfate) detector at resolution 4 cm^{-1}, 64 scans and Happ-Genzel appodization.

Raman spectra were collected using a Thermo Scientific DXR Raman microscope equipped with 532 nm line laser (power 0.1 mW) and 780 nm line (power 4 mW), respectively. The spot size of the lasers was focused by 50× objective. The scattered light was analyzed by a spectrograph with holographic gratings (900 and 1200 lines mm^{-1}), respectively, and a pinhole width of 50 μm. The acquisition time was 10 s with 10 repetitions. Thermo Scientific Peak Resolve module of Omnic software has been used to fit the "D" and "G" bands of the Raman spectra with the Gaussian profile.

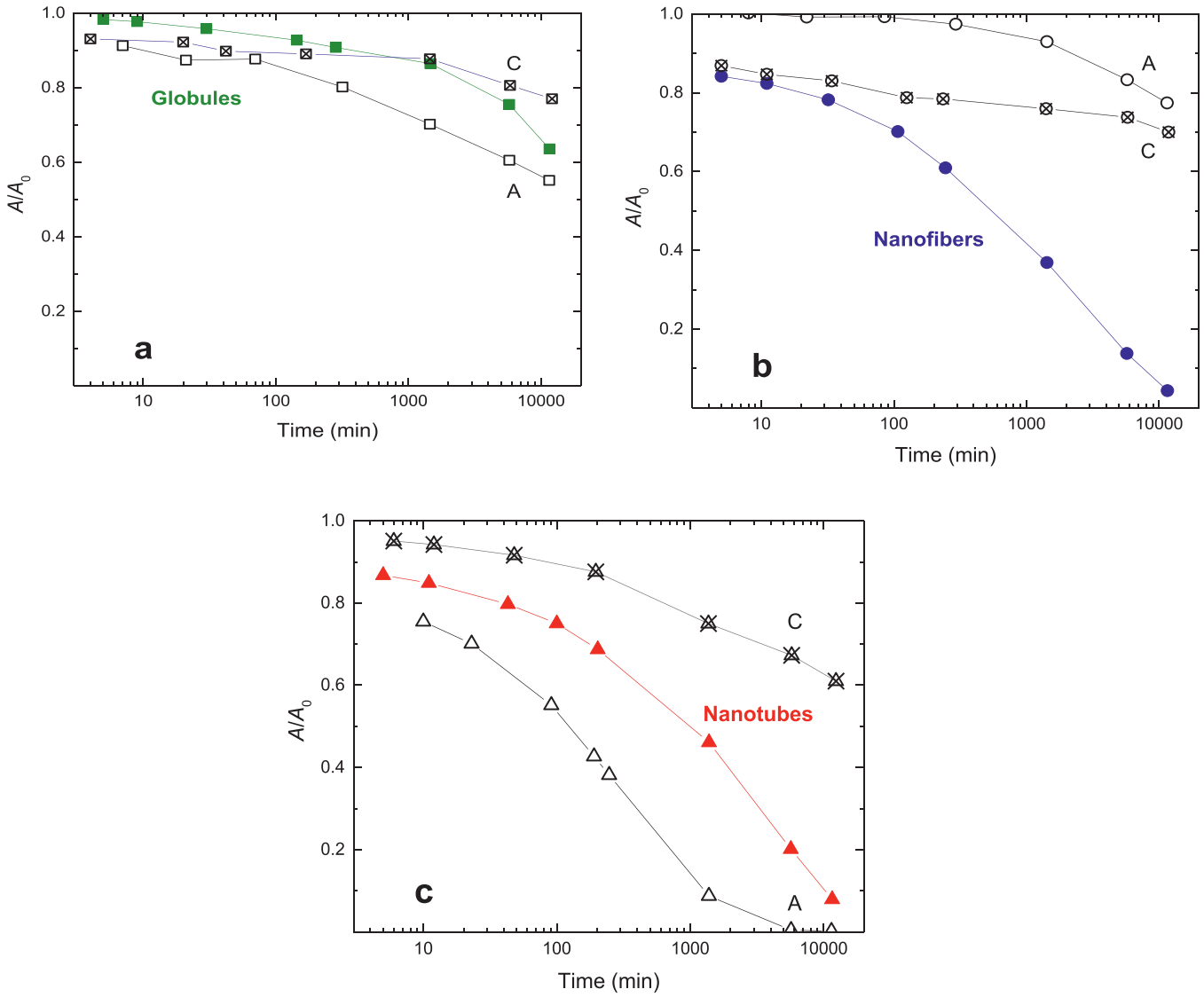

Fig. 6. Time dependence of the relative decrease in optical absorption A/A_0 of Reactive Black 5 solution at 596 nm wavelength in the presence of polypyrrole (a) globules, (b) nanofibres and (c) nanotubes (full symbols), products of their carbonization (650 °C, crossed symbols) and activation at the same temperature (A, open symbols). Dye concentration 1 g L^{-1}, 50 mg of adsorbent per 50 mL of dye solution, 20 °C. Data for the non-activated polypyrroles were taken from [4].

Specific surface area and pore volume were determined from adsorption and desorption isotherms with a NOVA3200 (Quantachrome Instruments) using a NovaWin software. Samples were degassed for 24 h at 100 °C, then adsorption and desorption isotherms were recorded with nitrogen (Linde, 99.999 %). Brunauer-Emmett-Teller analysis has been applied for the total surface area determination and Barrett-Joyner-Halenda (BJH) model for pores volume. Each sample was characterized four times with experimental error of 5%.

The conductivity was determined by four-point van der Pauw method on the powders compressed at 10 MPa in a lab-made cylindrical glass cell with inner diameter of 10 mm between an insulating support and a glass piston carrying four platinum/rhodium electrodes on the perimeter of its base. The setup included a Keithley 2010 miltimeter, a current source Keithley 220, and a Keithley 705 scanner equipped with a matrix card Keithley 7052. The pressure was controlled with a L6E3 load cell (Zemic Europe BV, The Netherlands). The dependence of the conductivity on the applied pressure was recorded at the same time.

2.4. Dye adsorption

Anionic dye, Reactive Black 5 (Sigma-Aldrich), has been selected as sorbate. The 50 mg portions of activated polypyrroles were suspended in 50 mL of the dye solution in water (100 mg L^{-1}) at room temperature and occasionally gently stirred. The dye/adsorbent mass ratio was 0.1. UV–vis spectra of the dye solution were recorded in dependence on time in 0.2 cm quartz cell with a Perkin-Elmer Lambda 20 UV–vis spectrometer. The dried activated polypyrrole with adsorbed dye was analyzed with FTIR and Raman spectroscopies.

3. Results and discussion

3.1. Morphology

It has been established in the literature that the carbonization of conducting polymers retains their original morphology except for some shrinkage [4,15,16]. The same applies to the activation of polypyrroles (Fig. 1).

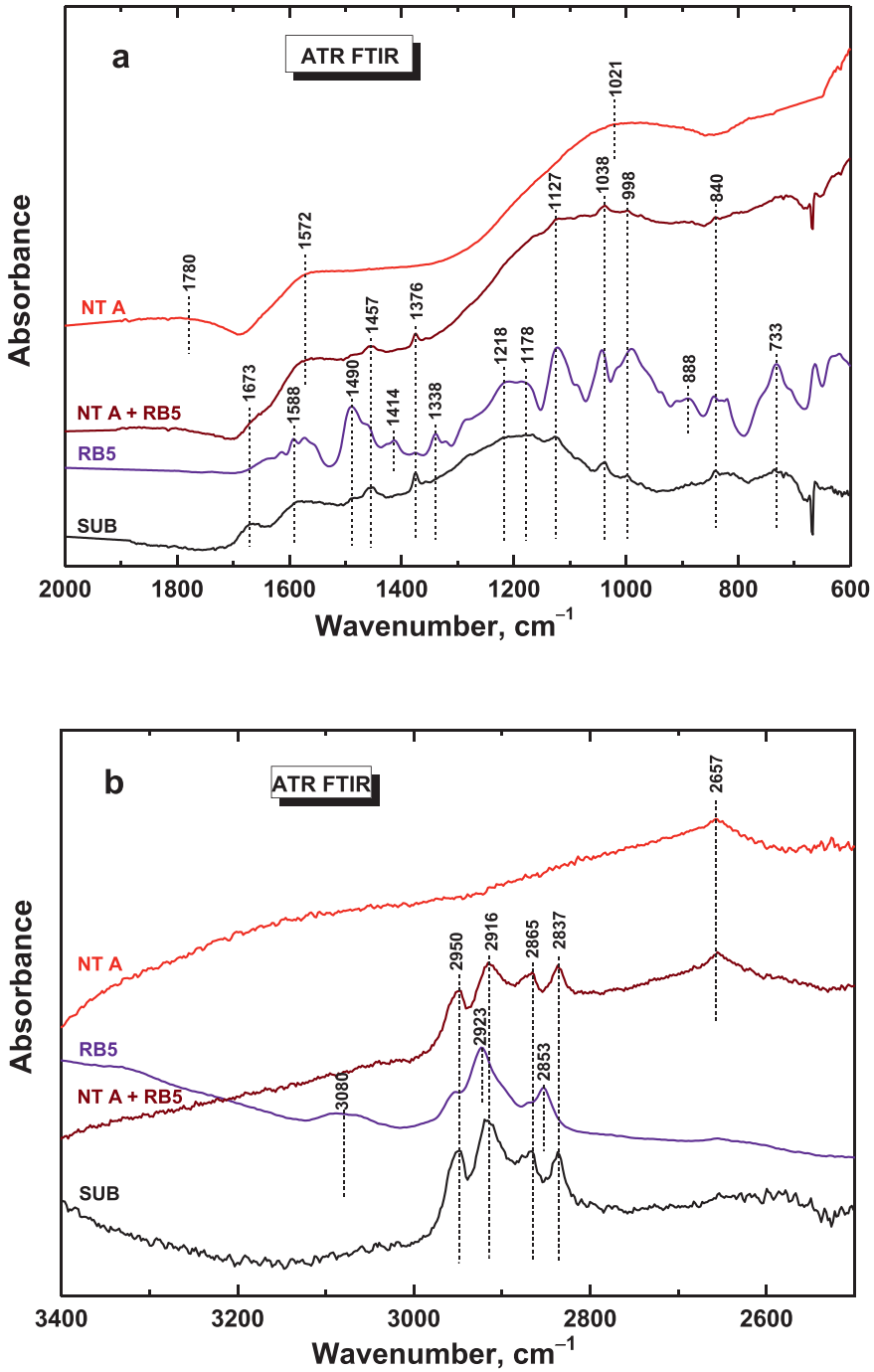

Fig. 7. ATR FTIR spectrum of activated polypyrrole nanotubes (NT A), activated nanotubes with adsorbed Reactive Black 5 (NT A+RB5), Reactive Black 5 (RB5), and subtraction spectrum SUB (NT A+RB5 minus NT A). (a) Lower and (b) higher wavenumber region.

3.2. FTIR spectra

The ATR FTIR spectrum of globular polypyrrole exhibits the main bands with local maxima at 1532 cm^{-1} (C–C stretching vibrations in the pyrrole ring), 1400 cm^{-1} (C–N stretching vibrations in the ring), 1284 cm^{-1} (C–H or C–N in-plane deformation modes), 1145 and 1090 cm^{-1} (breathing vibrations of the pyrrole rings), at 1043 and 999 cm^{-1} (C–H and N–H in-plane deformation vibrations) and the peaks located at 964 and 847 cm^{-1} (C–H out-of-plane deformation vibrations of the ring) [2,30]. The positions of maxima of these bands are only slightly shifted in the spectra of nanofibers and nanotubes (Fig. 2).

After carbonization at 650 °C in inert atmosphere, the spectra of all polypyrrole morphologies are transformed to the spectra of carbon-like materials (with two broad bands with maxima at 1574 cm^{-1} and 1145 cm^{-1}) [4]. The spectra of polypyrroles activated at the same temperature differ each from other. The spectrum of activated globular polypyrrole exhibits the maxima at 1585, 1195, 1054, and 913 cm^{-1}, for nanofibers at 1090 and 913 cm^{-1}, and for nanotubes at 1585 and 1054 cm^{-1}. This signifies that carbonization

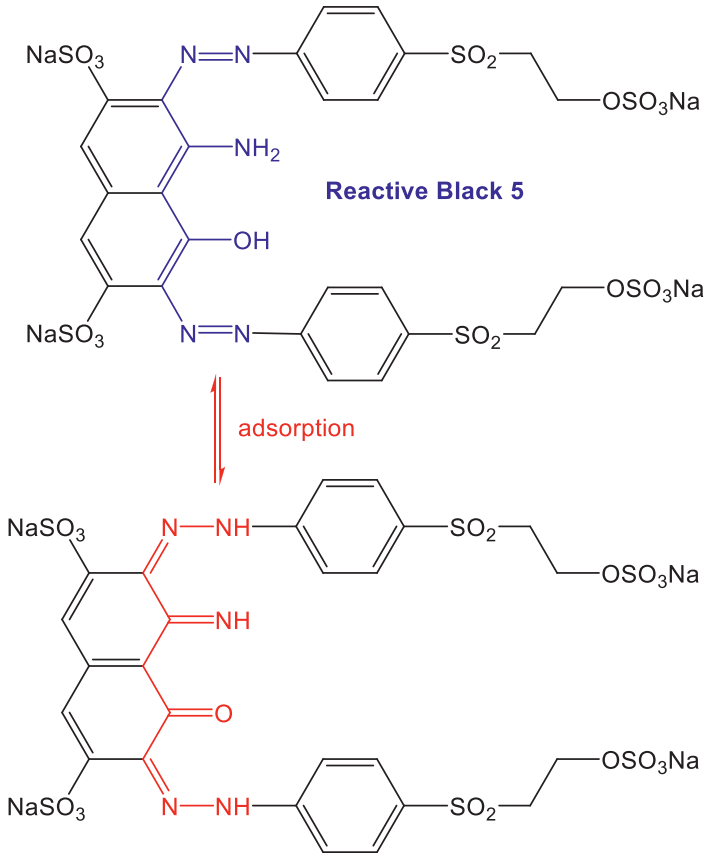

Fig. 8. The formula of Reactive Black 5 and its assumed adsorbed tautomer.

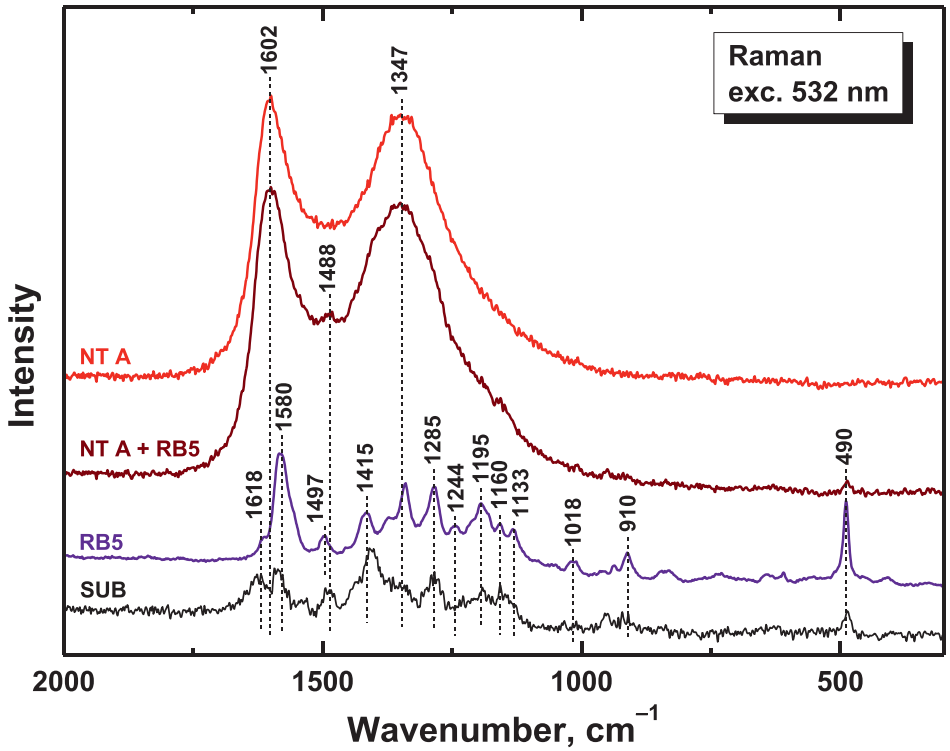

Fig. 9. Raman spectrum of activated polypyrrole nanotubes (NT A), the nanotubes with adsorbed dye (NT A+RB5), Reactive Black 5 (RB5), and subtraction spectrum SUB (NT A+RB5 minus NT A). Laser excitation wavelength 532 nm.

Table 1
The I_D/I_G ratios of integrated peak areas of "D" (disordered) and "G" (graphitic) bands of carbonized polypyrrole and activated analogues.

Morphology	I_D/I_G	
	Carbonized	Activated
Globular	7.7	3.4
Nanofibers	5.3	2.8
Nanotubes	4.5	3.5

Table 3
The conductivity (S cm^{-1}) of original, carbonized and activated polypyrroles of various morphologies determined at 10 MPa pressure.

Morphology	Original[a]	Carbonized[a]	Activated
Globular	0.24	0.0013	0.033
Nanofibers	9.6	0.029	0.015
Nanotubes	9.2	0.038	0.223

[a]The results for non-activated samples were taken from Ref. [4].

is not complete for activated samples and their structures contains some other groups.

3.3. Raman spectra

Raman spectra of polypyrroles carbonized at 650 °C in inert atmosphere [4] correspond to the characteristic Raman spectra of carbon-like materials with two broad bands with local maxima at 1562 and 1352 cm^{-1} (G- and D-bands) [20,31] (Fig. 3). They were observed in the infrared spectra due to the symmetry-breaking of the carbon network and the presence of nitrogen atom in the structure. These two broad bands are also present in the Raman spectra of activated samples, but they are sharper. Contrary to the infrared spectra, they are similar for all three tested morphologies and they are shifted to 1592 and 1315 cm^{-1} in comparison to their positions in the spectra of carbonized samples. The degree of structural disorder is characterized by the I_D/I_G ratios determined by the corresponding integrated peak areas in the Raman spectra (Table 1, Fig. 3). The lower values for activated samples may be due to better organized carbon-like part in their structure leading also to the higher conductivities (see below).

3.4. Specific surface area

Specific surface area is a key parameter for the applications of pollutant adsorbents or supercapacitors electrodes. The activation of polypyrrole, i.e. the carbonization in the presence of potassium hydroxide, is expected to increase the specific surface area of the resulting material. It has been applied to polypyrrole only exceptionally. Polypyrrole nanotubes had the specific surface area 5.38 m^2g^{-1}, which increased to 62.2 m^2g^{-1} and 92.6 m^2g^{-1} after activation. The higher values have been obtained when larger amount of potassium hydroxide was used [26]. Carbonized polypyrrole nanotubes had specific surface area 208 m^2g^{-1}, which increased after activation to 667–1226 m^2g^{-1} and total pore volume 0.23 cm^3g^{-1} to 0.51–0.68 cm^3g^{-1} [27].

The similar trend has been observed in the present case (Table 2, Fig. 4). Both one-dimensional morphologies have a higher specific surface area and pore volume compared to common globular. The surface area, however, does not increase after carbonization. This is in the contrast to the activation where the substantial increase was found both in surface areas and pore volumes (Fig. 4). This is due to the removal of the most of the organic part on molecular level resulting in the formation of nanopores, as it is also reflected by reduced yields.

3.5. Conductivity

The conductivity is a prime parameter for any conducting polymer, including its carbonized analogues. The superior conductivity of one-dimensional polypyrrole morphologies over globular polypyrrole prepared under comparable conditions reported in the literature [2] is well documented also in the present case (Table 3). This is explained by better ordering of polymer chains in one-dimensional morphologies, such as nanotubes and nanofibers. The conductivity became reduced after the carbonization by *ca* two orders of magnitude, and that of nanotubes was the highest (Table 3). This is in the correlation with the results of Raman spectroscopy (Table 1) indicating that the higher conductivity is associated with lower fraction of disordered phase. Despite the decreased conductivity, its level may be sufficient for applications, e.g., in supercapacitors [9,19] or in drug-delivery systems controlled by applied electric potential [32–35].

The conductivity partly recovered after the activation (Table 3) and the activated nanotubes provided the best result. Also here, the conductivity is in the correlation with the spectroscopic data (Table 1) suggesting again its inverse proportionality to the content of disordered phase. The dependence of the conductivity of powders on applied pressure could be monitored (Fig. 5). The slopes of the dependences in double-logarithmic presentation are comparable indicating also the similar mechanical properties of the activated samples.

3.6. Dye adsorption

The adsorption of organic dyes on carbonized polypyrrole nanotubes has been reported only rarely [19]. The adsorption capacities reached ≈500 mg g^{-1} for cationic dyes, methylene blue and Rhodamine G, but were lower, ≈100 mg g^{-1}, for anionic ones, Congo red and Orange G. For present study of activated polypyrroles, the adsorption of anionic azo dye, Reactive Black 5, was selected. This dye has recently been used in the adsorption studies on conducting polymers, polyaniline [36–38] and polypyrrole [4,39,40].

Table 2
Specific surface area and pore volume of polypyrroles and their carbonized and activated analogues[a]

Morphology	Specific surface area (m^2g^{-1})			Pore volume (cm^3g^{-1})		
	Original	Carbonized	Activated	Original	Carbonized	Activated
Globular	12.4±0.2	12.6±0.4	292±8.0	0.060±0.004	0.034±0.004	0.107±0.003
Nanofibers	65.1±2.1	87.0±3.7	229±2.0	0.240±0.077	0.290±0.001	0.160±0.004
Nanotubes	45.2±8.8	55.9±0.6	564±10	0.135±0.031	0.177±0.007	0.218±0.003

[a]The data for non-activated sampled are taken from Ref. [4].

Globular polypyrrole is a poor adsorbent of Reactive Black 5 dye and the only ca 40% of dye were adsorbed within two weeks allocated for the experiment (Fig. 6a). Neither carbonization nor activation improved the adsorption ability, despite the significantly increased specific surface area after the activation (Table 2). This suggests that the surface area is not a decisive factor in the adsorption process at original and carbonized samples. In the literature, activated globular polypyrrole was used as an adsorbent of 0.5–8 ppm methyl orange solutions [41]. The adsorption capacity 140 mg g^{-1} was reached within minutes. The dye concentrations, however, were considerably lower compared with experiments reported in this paper.

Polypyrrole nanofibers on the other hand proved to be an efficient adsorbent of a dye that could remove the dyes practically completely from the aqueous medium (Fig. 6b). The marked difference between the behavior or globules and nanofibers indicate that the morphology and chain-ordering constituting this morphology is a key factor controlling the adsorption efficiency. The reduced dye adsorption after the carbonization suggests the damage of ordered structure accompanied by the changes in molecular structure, which manifest themselves also in the reduced conductivity (Table 3). The same behavior is observed after the activation, when even the larger specific surface area cannot compensate the lost adsorption efficiency.

Polypyrrole nanotubes followed the same pattern as nanofibers, i.e. the original nanotubes adsorbed the dye nearly completely (Fig. 6c) and after the carbonization the adsorption decreased. In the deep contrast, however, activated nanotubes have been the most successful adsorbent among the tested samples, which even outperformed the original polypyrrole nanotubes. The activated nanotubes have been able to remove the dye completely.

3.7. Interaction of activated polypyrroles with the dye

To get insight in the molecular basis of the interaction between the studied materials and the dye, the ATR FTIR spectrum of Reactive Black 5 solution in the presence of activated polypyrrole nanotubes after drying has been compared with the spectrum of initial activated polypyrrole nanotubes and with Reactive Black 5 (Fig. 7). After adsorption of the dye from the solution to activated nanotubes, several new sharp peaks were identified. After subtraction of the spectrum of activated nanotubes without and with adsorbed dye, the overall shape of the spectrum is close to the spectrum of neat Reactive Black 5 (spectrum SUB in Fig. 7a) with the sharp peaks, which are better distinguished. Most of them are situated at the same positions as in the spectrum of dye. The intensity of the bands of aromatic ring C–C stretching vibrations 1588 and 1490 cm^{-1} relatively decreased, while a shoulder at 1457 cm^{-1} (most probably of the scissoring CH_2 vibrations) increased. This indicates the changes in the vicinity of the aromatic dye core (Fig. 8). Indeed, the peak of medium intensity situated at 1414 cm^{-1} (N=N stretching vibrations) and at 1338 cm^{-1} practically disappeared. This can be explained by the tautomeric keto–enol and related conversions of the dye structure (Fig. 8) as a consequence of the altered electron densities at the aromatic moiety caused by the adsorption on activated carbon.

In addition, the peak at 1376 cm^{-1} (possibly C–N stretching) has appeared. The bands with maxima at 1218, 1178, 1127, 1038, 998 cm^{-1} (region of stretching vibrations of SO_2 symmetrical and SO_3 stretching vibrations, and of CH in-plane bending vibrations) were detected in the spectrum of adsorbed dye. The bands at 840 and 733 cm^{-1} (NH wagging and CH out-of-plane bending vibrations) were also found in the spectrum of adsorbed dye [42,43]. A new band with maximum at 1673 cm^{-1} has been detected in the spectrum after subtraction which may be connected with the C=O stretching vibrations of keto- form in the adsorbed dye structure. In the region above 2500 cm^{-1} (Fig. 7b), the spectrum of neat Reactive Black 5 exhibits the band with a maximum at 3080 cm^{-1} (aromatic CH stretching vibrations), the peaks at 2923 cm^{-1} with a shoulder at 2950 (asymmetrical stretching vibrations of CH_2 group) and at 2853 cm^{-1} (symmetrical stretching vibrations of CH_2 group). In the spectrum of adsorbed dye they were observed at 2950, 2916 cm^{-1} and 2865, 2837 cm^{-1} [42,43]. These changes seem to be compatible with the conversion of tautomeric dye forms induced by the adsorption (Fig. 8).

Raman spectrum of Reactive Black 5 adsorbed on activated polypyrrole nanotubes has been compared with the spectrum of initial activated nanotubes and with Reactive Black 5 alone (Fig. 9). After the subtraction of the corresponding spectra, the spectra of original and adsorbed dye can be compared, the latter being well resolved (spectrum SUB). We detect the peaks at 1618, 1580 (with decreased intensity) and 1497 cm^{-1} (aromatic ring C–C stretching vibrations). A strong band with maximum at 1415 cm^{-1} corresponds most probably to the Raman active N=N stretching vibrations but its shift to lower wavenumbers supports the changes induced by the tautomerism (Fig. 8). The peaks at 1285, 1195, 1160 cm^{-1}, and sharp peak at 490 cm^{-1} are well detected in the spectrum of adsorbed dye. All the changes in the infrared and Raman spectra signify that an interaction between activated polypyrrole and Reaction Black 5 occurs with the support of tautomerism in the dye structure.

4. Conclusions

One-dimensional polypyrrole morphologies, nanofibers and nanotubes, dominate over the common globular form in conductivity, specific surface area and dye-adsorption ability. The typical conductivity of globular polypyrrole is of the order of 10^{-1} S cm^{-1}, for one-dimensional morphologies it is one order of magnitude higher. In the contrast to polypyrrole globules, both the nanofibers and nanotubes were able to remove the dye from aqueous solution practically completely. It is concluded the difference in polymer-chain ordering is responsible for this observation, the ordering in one-dimensional morphologies being more uniform.

The carbonization at 650 °C that converted polypyrrole to nitrogen-containing carbon generally reduced the conductivity by two orders of magnitude to 10^{-3}–10^{-2} S cm^{-1}. The higher conductivity correlates with the higher content of ordered phase as revealed by Raman spectroscopy. The specific surface area and pore volumes have not been practically affected. Dye adsorption on carbonized analogues was lower, as expected, due to the change in the molecular structure and limited possibility to create hydrogen or ionic bonds or establish π–π interaction that are responsible for the dye adsorption.

After the activation of polypyrroles at 650 °C, the morphology features were retained and the conductivity was partly recovered to 10^{-2}–10^{-1} S cm^{-1}. Both the specific surface areas and pore volumes increased several times, especially for nanotubes. Activated nanotubes also proved to be the best adsorbent among tested samples. Due to the uniform nanostructured morphology, activated polypyrrole nanotubes would make a material of choice for various applications. The low preparation yield, however, is a drawback.

It has to be stressed that the conclusions on dye adsorption concern a single anionic azo dye, an element of a large mosaic of organic dyes. For other types of dyes, the adsorption behavior might be quite different. The additional experiments are thus need to get the complete overview.

CRediT statement

Jaroslav Stejskal: Writing – original draft. Funding acquisition. **Miroslava Trchová:** Conceptualization. Writing – review &

editing. Methodology. **Ladislav Lapčák:** Data curation. Investigation. **Zdeňka Kolská:** Investigation. Formal analysis. **Miroslav Kohl:** Methodology. Resources. **Michal Pekárek:** Investigation. **Jan Prokeš:** Investigation. Validation.

Declaration of Competing Interest

The authors declare that they have no known competing financial interest or personal relationship that could have appeared to influence the work reported in this study.

Acknowledgment

The support of the Czech Science Foundation (19-04859S) is gratefully acknowledged.

Supplementary materials

Supplementary material associated with this article can be found, in the online version, at doi:10.1016/j.cartre.2021.100068.

References

[1] AL Pang, A Arsad, M. Ahmadipour, Synthesis and factor affecting on the conductivity of polypyrrole: a short review, Polym. Adv. Technol. 32 (2021) 1428–1454, doi:10.1002/pat.5201.
[2] J Stejskal, M. Trchová, Conducting polypyrrole nanotubes: a review, Chem. Pap. 72 (2018) 1563–1595, doi:10.1007/s11696-018-0394-x.
[3] J Stejskal, J. Prokeš, Conductivity and morphology of polyaniline and polypyrrole prepared in the presence of organic dyes, Synth. Met. 264 (2020) 116373, doi:10.1016/j.synthmet.2020.116373.
[4] J Stejskal, M Kohl, M Trchová, Z Kolská, M Pekárek, I Křivka, J. Prokeš, Conversion of conducting polypyrrole nanostructures to nitrogen-containing carbons and its impact on the adsorption of organic dye, Mater. Adv. 2 (2021) 706–717, doi:10.1039/d0ma00730g.
[5] XM Yang, ZX Zhu, TY Dai, Y. Lu, Facile fabrication of functional polypyrrole nanotubes via a reactive self-degraded template, Macromol. Rapid Commun. 26 (2005) 1736–1740, doi:10.1002/marc.200500514.
[6] I Sapurina, J Stejskal, I Šeděnková, M Trchová, J Kovářová, J Hromádková, J Kopecká, M Cieslar, A Abu El-Nasr, MM Ayad, Catalytic activity of polypyrrole nanotubes decorated with noble-metal nanoparticles and their conversion to carbonized analogues, Synth. Met. 214 (2016) 14–22, doi:10.1016/j.synthmet.2016.01.009.
[7] MC Wu, TS Zhao, RH Zhang, L Wei, HR. Jiang, Carbonized tubular polypyrrole with a high activity for the Br_2/Br^- redox reaction in zinc-bromine flow batteries, Electrochim. Acta 284 (2018) 569–576, doi:10.1016/j.electacta.2018.07.192.
[8] A Kannan, S. Radhakrishnan, Fabrication of an electrochemical sensor based on gold nanoparticles functionalized polypyrrole nanotubes for highly sensitive detection of L-dopa, Mater. Today Commun. 25 (2020) 101330, doi:10.1016/j.mtcomm.2020. 101330.
[9] BGS Raj, TH Ko, J Acharya, MK Seo, MS Khil, HY Kim, BS. Kim, A novel Fe_2O_3-decorated N-doped CNT porous composites derived from tubular polypyrrole with excellent rate capability and cycle stability as advanced supercapacitor anode materials, Electrochim. Acta 334 (2020) 135627, doi:10.1016/j.electacta.2020.135627.
[10] PF Shi, C Wang, JY Sun, P Lin, XT Xu, T. Yang, Thermal conversion of polypyrrole nanotubes to nitrogen-doped carbon nanotubes for efficient water desalination using membrane capacitive deionization, Sep. Purif. Technol. 235 (2020) 116196, doi:10.1016/j.seppur.2019.116196.
[11] J Upadhyay, TM Das, R Borah, K. Acharya, Electrochemical performance evaluation of polyaniline nanofibers and polypyrrole nanotubes, Mater. Today Proc. 32 (2020) 274–279, doi:10.1016/j.matpr.2020.01.370.
[12] YM Li, YY Gao, Q Zhang, RY Wang, CJ Li, JF Mao, LM Guo, FJ Wang, Z Zhang, L. Wang, Flexible and free-standing pristine polypyrrole membranes with a nanotube structure for repeatable Cr(VI) ion removal, Sep. Purif. Technol. 258 (2021) 117981, doi:10.1016/j.seppur.2020.117981.
[13] P Bober, Y Li, U Acharya, Y Panthi, J Pfleger, P Humpolíček, M Trchová, J. Stejskal, Acid Blue dyes in polypyrrole synthesis: the control of polymer morphology at nanoscale in the promotion of high conductivity and the reduction of cytotoxicity, Synth. Met. 237 (2018) 40–49, doi:10.1016/j.synthmet.2018.01.010.
[14] IM Minisy, U Acharya, L Kobera, M Trchová, C Unterweger, S Breitenbach, J Brus, J Pfleger, J Stejskal, P. Bober, Highly conducting 1-D polypyrrole prepared in the presence of safranin, J. Mater. Chem. C 8 (2020) 12140–12147, doi:10.1039/d0tc02838.
[15] G Ćirić-Marjanović, I Pašti, N Gavrilov, A Janosević, S. Mentus, Carbonised polyaniline and polypyrrole: towards advanced nitrogen-containing carbon materials, Chem. Pap. 67 (2013) 781–813, doi:10.2478/s11696-013-0312-1.
[16] M Trchová, EN Konyushenko, J Stejskal, J Kovářová, G. Ćirić-Marjanović, The conversion of polyaniline nanotubes to nitrogen-containing carbon nanotubes and their comparison with multi-walled carbon nanotubes, Polym. Degrad. Stab. 94 (2009) 929–938, doi:10.1016/j.polymdegradstab.2009.03.001.
[17] SM Shang, XM Yang, XM. Tao, Easy synthesis of carbon nanotubes with polypyrrole nanotubes as the carbon precursor, Polymer 50 (2009) 2815–2818, doi:10.1016/j.polymer.2009.04.041.
[18] J Kopecká, M Mrlík, R Olejník, D Kopecký, M Vrňata, J Prokeš, P Bober, Z Morávková, M Trchová, J. Stejskal, Polypyrrole nanotubes and their carbonized analogs: Synthesis, characterization, gas sensing properties, Sensors 16 (2016) 1917, doi:10.3390/s16111917.
[19] SC Xin, N Yang, F Gao, J Zhao, L Li, C. Teng, Three-dimensional polypyrrole-derived carbon nanotube framework for dye adsorption and electrochemical supercapacitor, Appl. Surf. Sci. 414 (2017) 218–223, doi:10.1016/j.apsusc.2017.04.109.
[20] G Ćirić-Marjanović, S Mentus, I Pašti, N Gavrilov, J Krstić, J Travas-Sejdic, LT Strover, J Kopecká, Z Morávková, M Trchová, J. Stejskal, Synthesis, characterization, and electrochemistry of nanotubular polypyrrole and polypyrrole-derived carbon nanotubes, J. Phys. Chem. C 118 (2014) 14770–14784, doi:10.1021/jp502862d.
[21] C Zhang, B Ma, YK. Zhou, Three-dimensional polypyrrole derived N-doped carbon nanotube aerogel as a high-performance metal-free catalyst for oxygen reduction reaction, ChemCatChem 11 (2019) 5495–5504, doi:10.1002/cctc.201901334.
[22] TS Hui, MAA. Zaini, Potassium hydroxide activation and activated carbon: a commentary, Carbon Lett. 16 (2015) 275–280, doi:10.5714/CL.2015,16.4.275.
[23] T Pan, HY liu, GY Ren, YN Li, XY Lu, Y. Zhu, Metal-free porous nitrogen-doped carbon nanotubes for enhanced oxygen reduction and evolution reactions, Sci. Bull. 61 (2016) 889–896, doi:10.1007/s11434-016-1073-3.
[24] DJ Xiao, J Ma, CL Chen, QM Luo, J Ma, LR Zheng, X. Zuo, Oxygen-doped carbonaceous polypyrrole nanotubes-supported Ag nanoparticle as electrocatalyst for oxygen reduction reaction in alkaline solution, Mater. Res. Bull. 105 (2018) 184–191, doi:10.1016/j.materresbull.2018.04.030.
[25] J Lin, YL Xu, J Wang, BF Zhang, D Li, C Wang, YL Jin, JB. Zhu, Nitrogen-doped hierarchically porous carbonaceous nanotubes for lithium ion batteries (2018), Chem. Eng. J. 352 (2018) 964–971, doi:10.1016/j.cej.2018.06.057.
[26] WL Wei, P. Liu, Rational porous design for carbon nanotubes derived from tubular polypyrrole as host for lithium-sulfur batteries, Micropor. Mesopor. Mater. 311 (2021) 110705, doi:10.1016/j.micromeso.2020.110705.
[27] CX Guo, N Li, LL Ji, YW Li, XM Yang, Y Lu, YF Tu, N- and O-doped carbonaceous nanotubes from polypyrrole for potential application in high-performance capacitance, J. Power Sources 247 (2014) 660–666, doi:10.1016/j.jpowsour.2013.09.014.
[28] Y Li, P Bober, M Trchová, J. Stejskal, Polypyrrole prepared in the presence of methyl orange and ethyl orange: nanotubes versus globules in the conductivity enhancement, J. Mater. Chem. C 5 (2017) 4236–4245, doi:10.1039/c7tc00206h.
[29] I Sapurina, Y Li, E Alekseeva, P Bober, M Trchová, Z Morávková, J. Stejskal, Polypyrrole nanotubes: the tuning of morphology and conductivity, Polymer 113 (2017) 247–258, doi:10.1016/j.polymer.2017.02.064.
[30] J Stejskal, I Sapurina, J Vilčáková, M Jurča, M Trchová, Z Kolská, J Prokeš, I. Křivka, One-pot preparation of conducting melamine/polypyrrole/magnetite ferrosponge, ACS Appl. Polym. Mater. 3 (2021) 1107–1115, doi:10.1021/acsapm.0c01331.
[31] MS Dresselhaus, G Dresselhaus, A. Jorio, Raman spectroscopy of carbon nanotubes in 1997 and 2007, J. Phys. Chem. C 111 (2007) 17887–17893, doi:10.1021/jp071378n.
[32] LM Lira, SI Córdoba de Torresi, Conducting polymer–hydrogel composites for electrochemical release devices: synthesis and characterization of semi-interpenetrating polyaniline–polyacrylamide networks, Electrochem. Commun. 7 (2005) 717–723, doi:10.1016/j.elecom.2005.04.027.
[33] M Bansal, A Dravid, Z Aqrawe, J Montgomery, ZM Wu, D. Svirskis, Conducting polymer hydrogels for electrically responsive drug delivery, J. Control. Rel. 328 (2020) 192–209, doi:10.1016/j.jconrel.2020.08.051.
[34] M Caldas, AC Santos, R Rebelo, I Pereira, F Veiga, RL Reis, VM. Correlo, Electro-responsive controlled drug delivery from melanin, Int. J. Pharm. 558 (2020) 119773, doi:10.1016/j.ijpharm.2020.119773.
[35] NR Jalal, T Madrakian, A Afkhami, A. Ghoorchian, Graphene oxide nanoribbons/polypyrrole nanocomposite film: controlled release of leucovorin by electrical stimulation, Electrochim. Acta 370 (2021) 137806, doi:10.1016/j.electacta.2021.137806.
[36] N Ballav, S Debnath, K Pillay, A. Maity, Efficient removal of Reactive Black from aqueous solution using polyaniline coated ligno-cellulose as a potential adsorbent, J. Mol. Liq. 209 (2015) 387–396, doi:10.1016/j.molliq.2015.05.051.
[37] P Bober, IM Minisy, U Acharya, J Pfleger, V Babayan, N Kazantseva, J Hodan, J. Stejskal, Conducting polymer composite aerogel with magnetic properties for organic dye removal, Synth. Met. 260 (2020) 116266, doi:10.1016/j.synthmet.2019.116266.
[38] J. Stejskal, Interaction of conducting polymers, polyaniline and polypyrrole, with organic dyes: polymer morphology control, dye adsorption and photocatalytic decomposition, Chem. Pap. 74 (2020) 1–54, doi:10.1007/s11696-019-00982-9.
[39] V. Janaki, K. Vijayaraghavan, B.T. Oh, A.K. Ramasamy, S. Kamala-Kannan, Synthesis, characterization and application of cellulose/polyaniline nanocomposite for the treatment of simulated textile effluent, Cellulose 20 (2013) 1153–1166, doi:10.1007/s10570-013-9910-x.
[40] PE Diaz-Flores, Ovando-Medina VM Guzmán-Alvárez, H Martínez-Gutiérrez, Ortega González, Synthesis of α-cellulose/magnetite/polypyrrole composite for the removal of reactive black 5 dye from aqueous solutions, Desalin. Water Treat. 155 (2019) 350–363, doi:10.5004/dwt.2019.24013.

[41] AA Alghamdi, AB Al-Odayni, WS Saeed, FA Almutairi, FA Alharthi, T Aouak, A Al-Kahtani, Adsorption of azo dye methyl orange from aqueous solutions using alkali-activate polypyrrole-based graphene-oxide, Molecules 24 (2019) 3685, doi:10.3390/molecules24203685.

[42] RM Silverstein, GC Bassler, TC. Morrill, Spectrometric Identification of Organic Compounds, 5th ed., Wiley, New York, 1991.

[43] G. Socrates, Infrared and Raman Characteristic Group Frequencies, 3rd ed., Wiley, New York, 2001.